Measurement and Modeling of Bubble and Dew Points of the Carbon Dioxide + Tetrahydrofuran + Water System

Khalik M. Sabil,[†,‡,§] Geert-Jan Witkamp,[†,||] and Cor J. Peters*[,†,⊥]

Process Equipment, Mechanical, Maritime & Materials Engineering, Delft University of Technology, Leeghwaterstraat 44, 2628 CA Delft, The Netherlands, Chemical Engineering Programme, Universiti Teknologi PETRONAS, Bandar Seri Iskandar, 31750 Tronoh, Perak, Malaysia, and Chemical Engineering Program, Bu Hasa Building, Room 2203, The Petroleum Institute, P.O. Box 2203, Abu Dhabi, United Arab Emirates

The bubble- and dew- point behavior of the carbon dioxide (1) + tetrahydrofuran (2) + water (3) system has been studied. Pressure−temperature isopleths were measured for the ternary system at $x_1 = 0.01$, 0.02, 0.03, 0.04, 0.09, and 0.27 at a constant mole fraction of tetrahydrofuran, $x_2 = 0.05$. The bubble- and dew-point lines for the ternary systems were also measured at $x_2 = 0.01$, 0.03, 0.05, and 0.07 for fixed composition of carbon dioxide (x_1) at 0.04 mol fraction and at $x_2 = 0.01$, 0.03, 0.05, 0.06, and 0.09 for a fixed composition of carbon dioxide (x_1) at 0.09, respectively. The pressure and temperature range from (1 to 6) MPa and (280 to 300) K, respectively. The experimental results for the ternary system have been modeled using the predictive Peng−Robinson−Stryjek−Vera (PRSV) equation of state with the Huron−Vidal−Orbey−Sandler (HVOS) mixing rule and the universal quasi-chemical activity coefficient (UNIQUAC) G^E model. Excellent agreements have been found between the experimental and the predicted values of the bubble and dew points of the ternary system throughout the composition range studied.

Introduction

Interest in ternary systems consisting of carbon dioxide, a polar organic solvent, and water arises from several technological needs. On the one hand, carbon dioxide and water mixtures are known to form clathrate hydrate.[1] It was established that certain soluble organic compounds such as tetrahydrofuran (THF), acetone, and 1,4-dioxane promote gas hydrate formation,[2] that is, these compounds showed to have a pressure-decreasing effect on the gas hydrate equilibrium pressure. This has led to several possibilities for the development of hydrate-based processes at moderate temperature and pressure conditions such as the pre- and post- combustion of carbon dioxide and carbon dioxide hydrate slurry as secondary refrigerants.[3,4] On the other hand, the addition of a polar organic cosolvent to a water + organic biphasic system, coupled with a subsequent phase splitting induced by the dissolution of carbon dioxide, creates an opportunity to run homogeneous reactions in an organic + aqueous mixture with a water-soluble catalyst, which may offer better activity and selectivity while allowing for high catalyst recovery.[5] Although the liquid−liquid phase split in a ternary system of carbon dioxide + organic + water systems may favor the reaction processes with homogeneous catalysts, the same effect might impede the development of hydrate-based process. If the hydrate-based processes are operated in the region where two liquid phases exist, an increase in operational and equipment costs is projected to ensure proper mixing of the liquids for hydrate formation, which make the processes becoming more expensive and less attractive. In worst case scenario, the desired hydrate formation may be hindered by the formation of the two liquid phases.

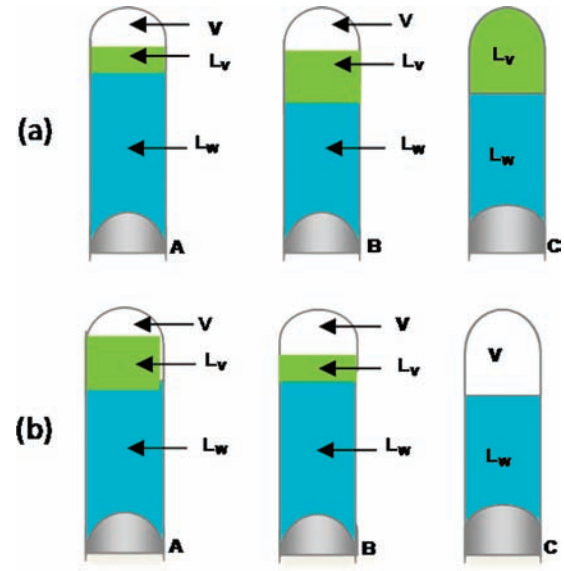

Figure 1. Schematic representation of a fluid phase transition: (a) bubble and (b) dew points.

In all cases mentioned above, the design and development of the processes require accurate knowledge of the phase behavior of the multicomponent systems. In all cases, the knowledge of the bubble- and dew-point data of the ternary systems is crucially important to determine the proper temperature and pressure conditions and the composition of each component at which the selected process will run successfully. For example, in the reaction processes, the bubble- and dew-point data will determine the region at which a miscibility switch will appear while in the hydrate-based processes. These data

* Corresponding author. Tel.: + 31 (0) 15 2782660 and +971 2 607 5492. Fax: +31 (0) 15 27 86975. E-mail: c.j.peters@tudelft.nl and cpeters@pi.ac.ae.
[†] Delft University of Technology.
[‡] Universiti Teknologi PETRONAS.
[§] E-mail: k.sabil@tudelft.nl.
[||] E-mail: g.j.witkamp@xs4all.nl.
[⊥] The Petroleum Institute.

10.1021/je900476e CCC: $40.75
Published on Web 09/10/2009

Table 1. List of Chemicals Used

component	purity	supplier	phase
H_2O	distilled and demineralized	own	liquid
CO_2	99.95 %	Messer-Griesheim	gas
THF	99.95 %	Sigma-Aldrich	liquid

Table 2. Pure Component Parameters for the PRSV EoS

compound	T_c/K	P_c/MPa	ω	k_1	r	q
CO_2	304.21	7.36	0.2250	0.04285	1.299	1.292
H_2O	647.13	22.055	0.3438		0.920	1.400
THF	540.15	5.19	0.2255	0.03961	2.866	2.172

Table 3. Energy Parameters Used in the HVOS Mixing Rule with the UNIQUAC G^E Model

	$-U_{12}$	U_{21}
system	J·mol^{-1}	J·mol^{-1}
H_2O (1) + THF (2)	$1.030T$/K − 371.4	$-2.272T$/K + 969.7
THF (1) + CO_2 (2)	$-3.154T$/K + 941.9	$4.081T$/K − 1250
H_2O (1) + CO_2 (2)	$-0.007397(T/\text{K})2$ + $4.122T$/K − 337.6	$-0.1579(T/\text{K})^2$ + $105.9T$/K − 17329

Table 4. $L_W-L_V-V \rightarrow L_W-L_V$ Transition (Bubble Point) for the Carbon Dioxide (1) + THF (2) + Water (3) System at a Fixed Mole Fraction of THF of 0.05 and Varied Carbon Dioxide Mole Fractions

T	P	T	P	T	P
K	MPa	K	MPa	K	MPa
$x_1 = 0.010$	$x_2 = 0.050$	$x_1 = 0.020$	$x_2 = 0.050$	$x_1 = 0.030$	$x_2 = 0.050$
282.45	1.35	282.47	2.22	282.20	2.48
284.45	1.42	285.47	2.32	286.52	2.67
286.45	1.52	288.47	2.41	289.52	2.80
287.44	1.53	290.45	2.47	290.45	2.84
289.50	1.56	291.41	2.51	291.45	2.88
291.45	1.63	292.43	2.53	292.51	2.92
293.43	1.71	293.48	2.57	293.50	2.97
295.43	1.79	294.42	2.60	295.44	3.05
297.49	1.88	295.47	2.63	297.43	3.14
299.41	1.94	297.47	2.69	299.42	3.22
		299.47	2.75	301.47	3.31
$x_1 = 0.040$	$x_2 = 0.050$	$x_1 = 0.090$	$x_2 = 0.050$	$x_1 = 0.270$	$x_2 = 0.050$
282.50	2.70	282.40	3.35	282.40	3.92
285.50	2.86	284.40	3.51	283.40	4.02
288.50	3.02	289.45	3.90	285.40	4.23
291.10	3.16	291.49	4.06	287.40	4.44
291.48	3.18	292.49	4.14	289.44	4.65
291.96	3.21	293.48	4.22	290.40	4.76
292.46	3.23	294.50	4.30	291.46	4.86
293.41	3.29	295.49	4.38	292.50	4.97
294.40	3.34	296.45	4.45	293.50	5.08
295.50	3.40	296.45	4.45	295.40	5.28
297.50	3.51	297.45	4.53	297.40	5.49
299.50	3.61	299.45	4.69	299.40	5.69

are prerequisites to model the hydrate phase behavior. In the literature, data for the system of THF + carbon dioxide + water have been reported at (298, 313, and 333) K for a pressure range of (1.03 to 5.17) MPa.[5] However, because of their method of measurement in which pressure and temperature were fixed, the effect of the different overall composition of each component on the liquid−liquid phase split cannot be determined. In the present work, the bubble-point and dew-point data for the ternary system of THF + carbon dioxide + water are determined experimentally for the different overall composition of each component in the system. Since the results of this work are focused toward application in carbon dioxide hydrate work, the overall mole fraction of carbon dioxide in the samples of the ternary system is kept below 0.01. Additionally, the experimental ternary results are modeled using the Peng−Robinson−Stryjek−Vera (PRSV) equation of state (EoS), combined with Huron−Vidal−Orbey−Sandler (HVOS) mixing rules. Experimental data and calculated results are compared and reported.

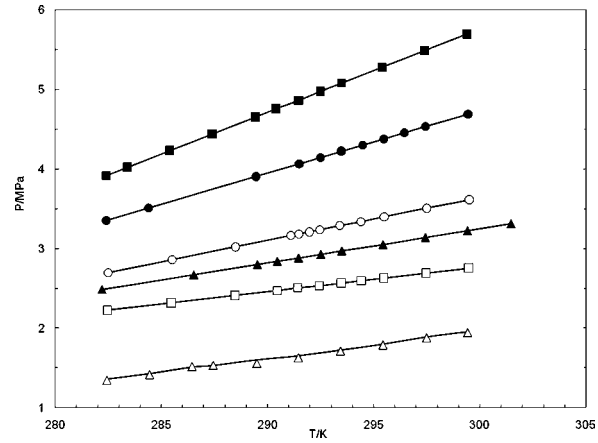

Figure 2. *P,T* projection of bubble points ($L_W-L_V-V \rightarrow L_W-L_V$) for the system CO_2 (1) + THF (2) + H_2O (3) at $x_2 = 0.05$ and different mole fractions of carbon dioxide: Δ, 0.01; □, 0.02; ▲, 0.03; ○, 0.04; ●, 0.09, ■, 0.27. The modeled data are represented by solid lines.

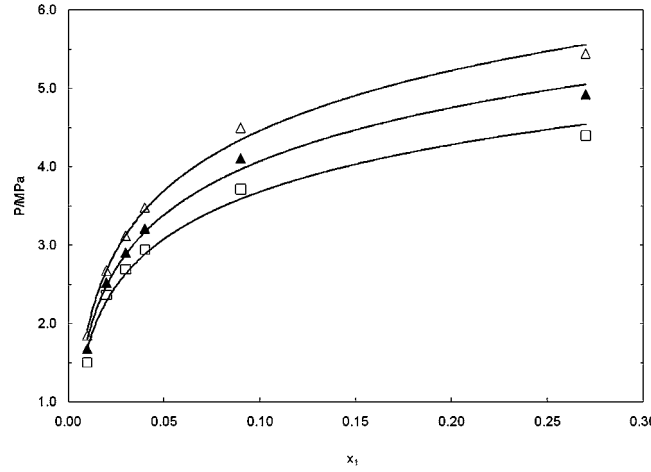

Figure 3. *P,x* section for bubble points ($L_W-L_V-V \rightarrow L_W-L_V$) at various temperatures for the CO_2 (1) + THF (2) + H_2O (3) system at $x_2 = 0.05$. The data that are calculated from the fitted isopleths are represented by markers: □, 287 K; ▲, 292 K; Δ, 297 K. The modeled data are represented by solid lines.

Experimental Section

Apparatus and Procedure. The hydrate equilibrium conditions of the systems containing water + carbon dioxide + an electrolyte + THF have been determined using the Cailletet apparatus. The Cailletet apparatus used in the present study works according to the static synthetic method. The essential part of the apparatus is a thick-walled capillary glass tube, known as a Cailletet tube, which acts as the equilibrium cell. Details of the apparatus can be found in Raessi and Peters.[6]

Filling the equilibrium cell (Cailletet tube) with the desired amounts of liquid and gaseous components was carried out with the aid of a "gas rack apparatus", equipped with a high vacuum turbo pump and an ionization vacuum meter. A known amount of aqueous solution (water + THF) was injected into the Cailletet tube. The composition of the aqueous solutions was predetermined. Then, the sample was outgassed with high vacuum while it was kept frozen with liquid nitrogen. Additional degassing of the liquid sample was achieved by successive freezing and melting the sample under high vacuum. A known amount of carbon dioxide was then dosed volumetrically at a known temperature and pressed into the tube using mercury. The capillary tube was then transferred to the Cailletet apparatus for the equilibrium measurements.

Table 5. $L_W-L_V-V \rightarrow L_W-L_V$ Transition (Bubble Point) for the Carbon Dioxide (1) + THF (2) + Water (3) System at a Fixed Mole Fraction of Carbon Dioxide of 0.04 and Varied THF Mole Fractions

T	P	T	P	T	P	T	P
K	MPa	K	MPa	K	MPa	K	MPa
$x_1 = 0.040$	$x_2 = 0.010$	$x_1 = 0.040$	$x_2 = 0.030$	$x_1 = 0.040$	$x_2 = 0.050$	$x_1 = 0.040$	$x_2 = 0.070$
282.45	4.01	282.46	3.29	282.45	2.69	282.45	2.22
284.45	4.20	285.45	3.49	284.50	2.81	285.45	2.35
286.45	4.40	287.45	3.62	286.50	2.91	287.45	2.43
288.45	4.59	289.46	3.76	289.50	3.07	289.48	2.52
289.46	4.69	290.46	3.82	291.10	3.16	290.54	2.56
290.51	4.79	291.45	3.89	291.48	3.18	291.44	2.60
291.45	4.87	292.45	3.96	291.96	3.21	292.40	2.64
292.51	4.98	293.44	4.02	292.46	3.23	293.43	2.68
293.50	5.08	295.45	4.16	293.41	3.29	295.43	2.77
295.50	5.27	297.45	4.29	294.40	3.34	297.43	2.85
297.50	5.46	299.45	4.43	295.50	3.40	299.40	2.94
299.50	5.65			297.50	3.51		
				299.50	3.61		

Table 6. $L_W-L_V-V \rightarrow L_W-L_V$ Transition (Bubble Point) for the Carbon Dioxide (1) + THF (2) + Water (3) System at a Fixed Mole Fraction of Carbon Dioxide of 0.09 and Varied THF Mole Fractions

T	P	T	P	T	P
K	MPa	K	MPa	K	MPa
$x_1 = 0.090$	$x_2 = 0.010$	$x_1 = 0.090$	$x_2 = 0.030$	$x_1 = 0.090$	$x_2 = 0.050$
282.50	4.02	282.50	3.51	282.45	3.36
284.51	4.24	284.50	3.69	283.45	3.43
286.51	4.45	286.50	3.87	285.45	3.59
288.51	4.67	288.50	4.06	287.45	3.75
289.50	4.77	290.49	4.24	289.45	3.90
290.52	4.87	291.52	4.34	291.49	4.06
291.57	4.98	292.44	4.42	292.49	4.14
292.56	5.09	293.42	4.51	293.48	4.22
293.57	5.20	295.42	4.69	294.50	4.30
295.50	5.40	297.42	4.87	295.49	4.38
295.57	5.41	299.42	5.06	296.45	4.45
299.57	5.83			297.45	4.53
				299.45	4.69
$x_1 = 0.090$	$x_2 = 0.060$	$x_1 = 0.090$	$x_2 = 0.090$		
282.45	3.18	282.43	2.58		
284.40	3.33	284.43	2.67		
285.45	3.41	286.43	2.77		
287.45	3.56	288.45	2.86		
289.45	3.70	290.38	2.96		
291.47	3.85	291.43	3.00		
292.49	3.93	292.43	3.05		
293.42	4.00	293.43	3.10		
295.42	4.15	294.44	3.16		
297.40	4.30	295.45	3.20		
299.42	4.45	297.45	3.30		
		299.43	3.39		

For the measurement of bubble-point curves, the temperature was fixed at a constant value, and the pressure was adjusted using the dead-weight pressure gauge. The starting point was at a pressure where a vapor phase (V), liquid water (L_W), and liquid organic (L_V) are present. From this point, the pressure was increased gradually until the last bubbles of the vapor phase disappear, that is, $L_W + L_V + V \rightarrow L_W + L_V$. Similarly, the starting point for the dew point measurements was the same. However, the pressure was reduced until the last droplets of the condensed gas phase disappear, that is, $L_W + L_V + V \rightarrow L_W + V$. For all types of phase transition measurements, the pressure was corrected for the pressure generated by the height of the mercury column and the atmospheric pressure as well. The schematic representation of the phase transitions are shown in Figure 1.

Materials. The chemicals used in the present study are listed in Table 1 with their purity and suppliers. Carbon dioxide and THF were used without any further purification.

Modeling

In the present work, the Peng−Robinson EoS with the modification by Stryjek and Vera (PRSV EoS) was used for the phase equilibrium calculations for the fluid phases with the HVOS mixing rule.[7,8] The excess Gibbs free energy required in the HVOS mixing rule was determined by using UNIQUAC

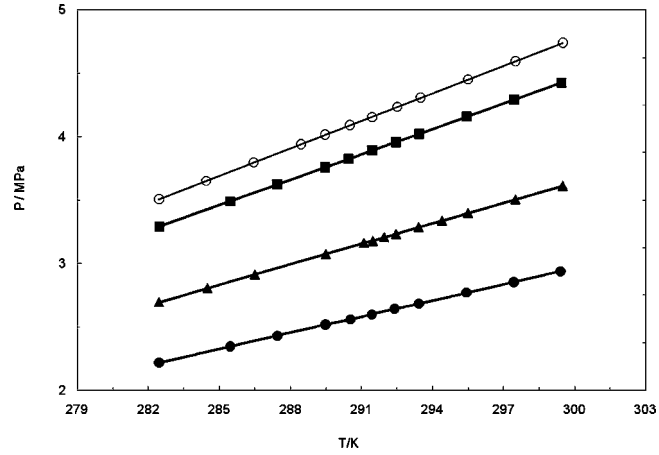

Figure 4. *P*,*T* projection of bubble points ($L_W-L_V-V \rightarrow L_W-L_V$) for the CO_2 (1) + THF (2) + H_2O (3) system at $x_1 = 0.04$ and different mole fractions of THF: ○, 0.01; ■, 0.03; ▲, 0.05; ●, 0.07. The modeled data are represented by solid lines.

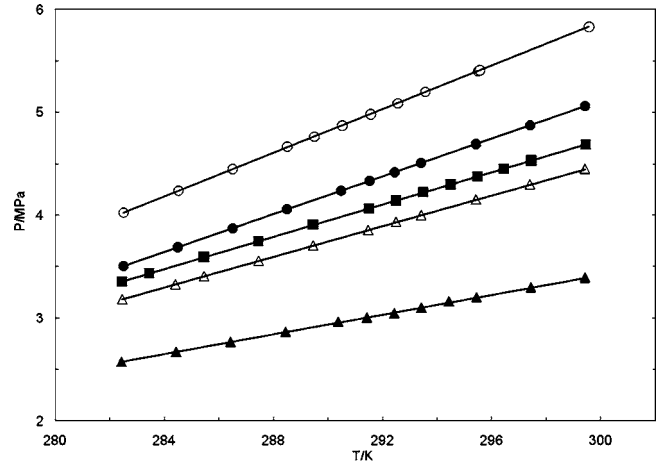

Figure 5. *P*,*T* projection of bubble points ($L_W-L_V-V \rightarrow L_W-L_V$) for the CO_2 (1) + THF (2) + H_2O (3) system at $x_1 = 0.09$ and different mole fractions of THF: ○, 0.01; ●, 0.03, ■, 0.05; Δ, 0.06; ▲, 0.09. The modeled data are represented by solid lines.

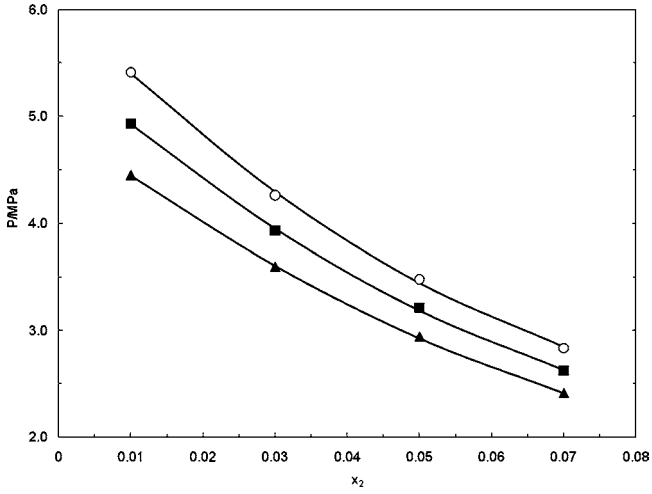

Figure 6. *P,x* section for bubble points ($L_W-L_V-V \rightarrow L_W-L_V$) at various temperatures for the CO_2 (1) + THF (2) + H_2O (3) system at $x_1 = 0.04$. The data that are calculated from the fitted isopleths are represented by markers: ▲, 287 K; ■, 292 K; ○, 297 K. The modeled data are represented by solid lines.

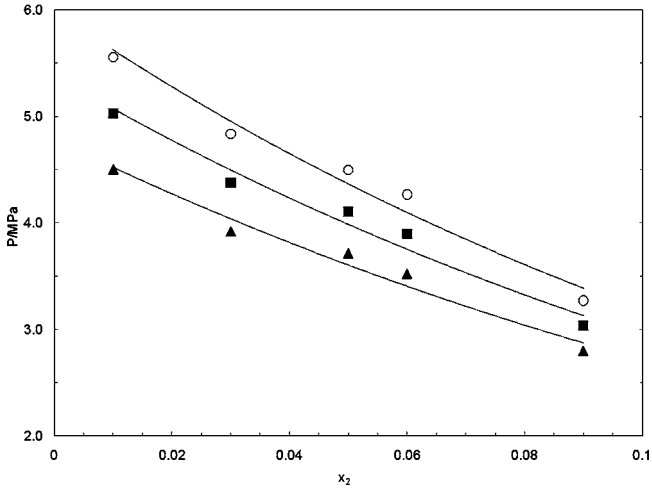

Figure 7. *P,x* cross section for bubble points ($L_W-L_V-V \rightarrow L_W-L_V$) at various temperatures for the CO_2 (1) + THF (2) + H_2O (3) system at $x_1 = 0.09$. The data that are calculated from the fitted isopleths are represented by markers: ▲, 287 K; ■, 292 K; ○, 297 K. The modeled data are represented by solid lines.

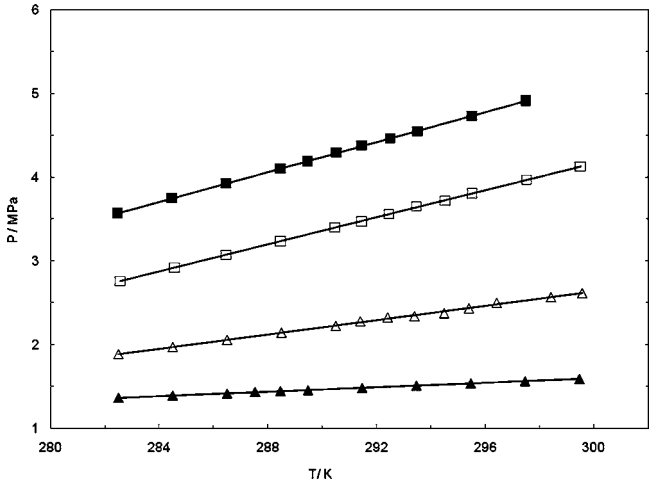

Figure 8. *P,T* projection of dew points ($L_W-L_V-V \rightarrow L_W-L_V$) for the CO_2 (1) + THF (2) + H_2O (3) system at $x_1 = 0.04$ and different mole fractions of THF: ■, 0.01; □, 0.03; Δ, 0.05; ▲, 0.07. The modeled data are represented by solid lines.

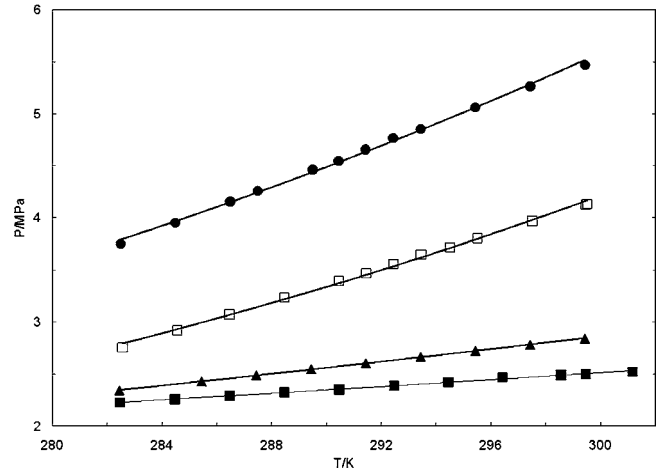

Figure 9. *P,T* projection of dew points ($L_W-L_V-V \rightarrow L_W-L_V$) for the CO_2 (1) + THF (2) + H_2O (3) system at $x_1 = 0.09$ and different mole fractions of THF: ●, 0.01; □, 0.03; ▲, 0.05; ■, 0.06. The modeled data are represented by solid lines.

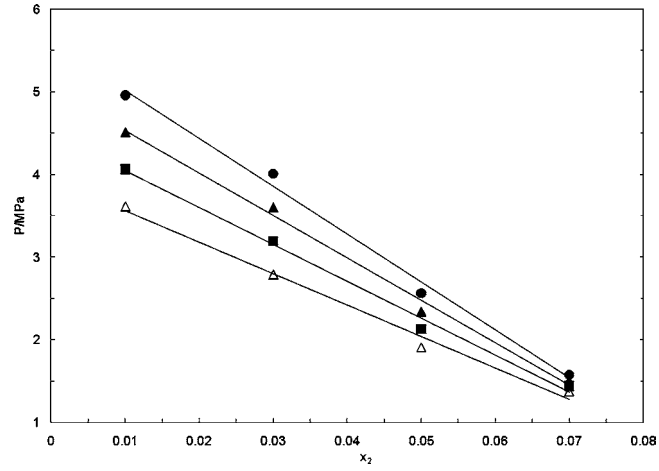

Figure 10. *P,x* projection of dew points ($L_W-L_V-V \rightarrow L_W-L_V$) for the CO_2 (1) + THF (2) + H_2O (3) system at $x_1 = 0.04$. The data that are calculated from the fitted isopleths are represented by markers: ●, 283 K; ▲, 288 K; ■, 293 K; Δ, 298 K. The modeled data are represented by solid lines.

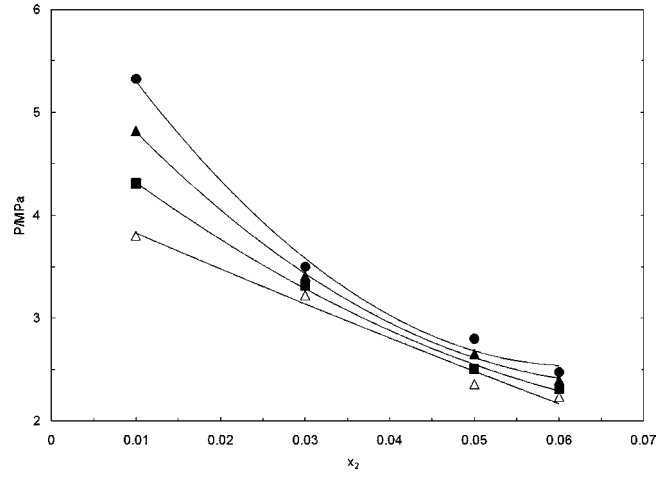

Figure 11. *P,x* projection of dew points ($L_W-L_V-V \rightarrow L_W-L_V$) for the CO_2 (1) + THF (2) + H_2O (3) system at $x_1 = 0.09$. The data that are calculated from the fitted isopleths are represented by markers: ●, 283 K; ▲, 288 K; ■, 293 K; Δ, 298 K. The modeled data are represented by solid lines.

(universal quasi-chemical activity coefficient) model. The pure component parameters for PRSV EoS together with UNIQUAC parameters were tabulated in Table 2. In this table, *r* is the

Table 7

T	P	T	P	T	P
K	MPa	K	MPa	K	MPa
$x_1 = 0.040$	$x_2 = 0.010$	$x_1 = 0.040$	$x_2 = 0.030$	$x_1 = 0.040$	$x_2 = 0.050$
282.46	3.57	282.56	2.76	282.49	1.89
284.46	3.75	284.56	2.92	284.49	1.97
286.46	3.93	286.46	3.07	286.49	2.06
288.46	4.10	288.46	3.23	288.49	2.14
289.46	4.19	290.46	3.40	290.49	2.22
290.51	4.29	291.45	3.47	291.39	2.28
291.45	4.38	292.44	3.56	292.40	2.32
292.50	4.46	293.45	3.65	293.39	2.34
293.50	4.55	294.51	3.72	294.48	2.37
295.50	4.73	295.51	3.81	295.39	2.43
297.50	4.91	297.51	3.97	296.41	2.50
299.50	5.09	299.46	4.13	298.41	2.57
		299.51	4.13	299.56	2.61

$x_1 = 0.040$	$x_2 = 0.070$
282.49	1.37
284.49	1.39
286.49	1.42
287.52	1.44
288.46	1.45
289.47	1.46
291.47	1.48
293.47	1.51
295.47	1.54
297.47	1.56
299.47	1.59

Table 8

T	P	T	P	T	P
K	MPa	K	MPa	K	MPa
$x_1 = 0.090$	$x_2 = 0.010$	$x_1 = 0.090$	$x_2 = 0.030$	$x_1 = 0.090$	$x_2 = 0.050$
282.49	3.75	282.44	3.21	282.47	2.23
284.49	3.95	285.44	3.27	284.47	2.26
286.49	4.16	287.44	3.30	286.47	2.29
287.49	4.26	289.44	3.34	288.47	2.32
289.49	4.46	291.44	3.38	290.47	2.35
290.44	4.55	292.44	3.40	292.47	2.39
291.43	4.66	293.44	3.42	294.45	2.42
292.43	4.77	294.45	3.43	296.43	2.47
293.43	4.85	296.45	3.47	298.55	2.49
295.43	5.06	297.45	3.49	299.47	2.50
297.43	5.26	299.45	3.53	301.17	2.52
299.43	5.47				

$x_1 = 0.090$	$x_2 = 0.060$
282.44	2.34
285.44	2.43
287.44	2.49
289.44	2.55
291.44	2.60
293.44	2.66
295.44	2.72
297.44	2.78
299.44	2.84

UNIQUAC pure component volume parameter, and q is the UNIQUAC pure component area parameter. The energy parameters, U_{ij}, for the G^E model were obtained by fitting the data obtained from Lazzaroni and co-workers.[5] The fitted equations were tabulated in Table 3.

Results and Discussion

For the bubble-point conditions ($L_W-L_V-V\rightarrow L_W-L_V$), the experimental data of the ternary system of carbon dioxide + THF + water together with the modeling results at a constant THF composition of 0.05 mole fraction in the aqueous solution are tabulated in Table 4 and visualized in Figure 2 as isopleths, that is, as loci for a constant overall composition. The mole fraction of carbon dioxide is varied from 0.01 to 0.27. To examine the consistency of the various isopleths, each isopleth of the ternary system is fitted to a second-order polynomial with an average correlation coefficient of 0.998. From the fitted function, the bubble-point pressure can be calculated for various values of the temperature as a function of the composition of the system as shown in Figure 3. As can be seen in Figures 2 and 3, the calculated and measured data are in good agreement throughout the temperature, pressure, and concentration ranges

studied. In general, the model slightly under-predicts the equilibrium pressure of the system at a specified overall concentration of carbon dioxide. The average absolute relative deviation (AARD) is found to be 3.7 %. The AARD is calculated as:

$$\mathrm{AARD} = \frac{1}{N_{\mathrm{exp}}} \sum_{i=1}^{N_{\mathrm{exp}}} \left(\frac{|P_{i,\mathrm{exp}} - P_{i,\mathrm{cal}}|}{P_{i,\mathrm{exp}}} \right) \quad (1)$$

Next, the measured and modeled bubble point conditions ($L_W-L_V-V \rightarrow L_W-L_V$) of the ternary system at an overall constant carbon dioxide mole fraction of 0.04 and 0.09 are tabulated in Tables 5 and 6 and are depicted as isopleths in Figures 4 and 5, respectively. The *P*,*x* section for both systems is constructed as previously discussed and represented together with the modeling results in Figures 6 and 7, respectively.

The calculated AARD % for both cases is 0.32 % and 2.6 %, respectively. The good agreement of the predicted isopleths and isotherm lines in all cases demonstrates the ability of the models to capture the bubble-point pressure dependencies on concentration and temperature. In general, as the temperature increased from (282 to 297) K, the bubble-point pressure is also increasing. With regard to the carbon dioxide concentration, the bubble-point pressure also increases with its concentration. In contrast, if the concentration of THF increases, the bubble-point pressure decreases. The lowering of the bubble-point pressure with the increasing amount of THF may be explained on the basis of the high solubility of carbon dioxide in THF.[9] The authors attributed the high solubility of carbon dioxide in THF to the possibility of carbon dioxide acting like a Lewis acid and thus being likely to interact with the basic ether functionality of THF; that is, the higher the amount of THF in the system, the easier it will be for carbon dioxide to dissolve in the liquid organic aqueous phase (L_V).

Similarly, the dew point lines ($L_W-L_V-V \rightarrow L_W-L_V$) for the ternary systems at different concentrations of THF and carbon dioxide are measured and modeled. Two systems with a fixed carbon dioxide concentration of 4 mol % and 9 mol % and varied THF concentration are presented in this work. The measured data are tabulated in Tables 7 and 8 and depicted in Figures 8 and 9, respectively. In addition, four isotherms for each system are represented in Figures 10 and 11.

Again, it is shown that the model used in the work is able to represent the phase boundary between all of the fluid phases of the systems studied with an AARD of 3.4 % and 1.8 % respective to the two examples used in this work. In general, the AARD is increasing with a decreasing mole fraction of carbon dioxide in the system. Both predicted and experimental results show that the carbon dioxide + THF + water system requires a very little amount of carbon dioxide for a liquid−liquid phase split to occur. The infinite dilution activity coefficient (γ^{∞}) of THF in water at 298 K measured by Sherman et al. is 17.01.[10] This value shows that, although THF is completely miscible in water, the system strongly deviates from ideality and, therefore, is susceptible to a phase split upon addition of carbon dioxide to the system. Moreover, it is clearly observed that the dew-point line is becoming more horizontal as the concentration of THF is increasing in the system. As the dew-point line is used to indicate the occurrence of a liquid−liquid phase split in the ternary system, the trend shows that the liquid phase is becoming more susceptible to a liquid−liquid phase split when higher amounts of THF are present in the system.

Conclusion

In the present work, we present measured data of bubble and dew points of the carbon dioxide + water + THF system at several compositions of carbon dioxide and THF in the ternary system, respectively. It was found that the bubble-point pressure of the system increases with the increase of carbon dioxide concentration and a decrease of THF concentration. The measured dew points show that the ternary system is subjected to a liquid−liquid phase split in the temperature and pressure ranges studied. The PRSV EoS is capable of accurately predicting the bubble- and dew-point curves for the ternary system studied using HVOS mixing rule.

Acknowledgment

The authors thank L.J. Florusse and E.J.M. Straver for their assistance in the experimental work.

Literature Cited

(1) Sloan, E. D.; Koh, C. A. *Clathrate Hydrate of Natural Gases*, 3rd ed.; CRC Press: Coral Gables, FL, 2007.
(2) de Deugd, R. M.; Jager, M. D.; de Swaan Arons, J. Mixed hydrates of methane and water-soluble hydrocarbons modeling of empirical results. *AIChE J.* **2001**, *47*, 693–704.
(3) Kang, S.-P.; Lee, H. Recovery of CO_2 from Flue Gas using Gas Hydrate: Thermodynamic Verification through Phase Equilibrium Measurements. *Environ. Sci. Technol.* **2000**, *34*, 4397–4400.
(4) Fournaison, L.; Delahaye, A.; Chatti, I.; Petitet, J.-P. CO_2 Hydrates in Refrigeration Processes. *Ind. Eng. Chem. Res.* **2004**, *43*, 6521–6526.
(5) Lazzaroni, M. J.; Bush, D.; Jones, R.; Hallett, J. P.; Liotta, C. I.; Eckert, C. A. High-Pressure Phase Equilibria of Some Carbon Dioxide-Organic-Water systems. *Fluid Phase Equilib.* **2004**, *224*, 143–154.
(6) Raeissi, S.; Peters, C. J. Experimental Determination of High-Pressure Phase Equilibria of the Ternary System Carbon Dioxide plus Limonene plus Linalool. *J. Supercrit. Fluids* **2005**, *35*, 10–17.
(7) Stryjek, R.; Vera, J. H. PRSV - An Improved Peng-Robinson Equation of State for Pure Compounds and Mixtures. *Can. J. Chem. Eng.* **1986**, *64*, 323–333.
(8) Orbey, H.; Sandler, S. I. On the combination of equation of state and excess free energy models. *Fluid Phase Equilib.* **1995**, *111*, 53–70.
(9) Lazzaroni, M. J.; Bush, D.; Brown, J. S.; Eckert, C. A. High-Pressure Vapor-Liquid Equilibria of Some Carbon Dioxide + Organic Binary Systems. *J. Chem. Eng. Data* **2005**, *50*, 60–65.
(10) Sherman, S. R.; Trampe, D. B.; Bush, D. M.; Schiller, M.; Eckert, C. A.; Dallas, A. J.; Li, J.; Carr, P. W. Compilation and Correlation of Limiting Activity Coefficients of Nonelectrolytes in Water. *Ind. Eng. Chem. Res.*, **1996**, *35*, 1044–1058.

Received for review June 5, 2009. Accepted August 21, 2009. The authors thank the Institute Technology PETRONAS (Ltd.), Malaysia for the financial assistance of the work.

JE900476E